Fano resonance of nanoparticles embedded in Fabry-Perot cavities

Jianhong Zhou,[1,*] Xiping Xu,[1] Wenbo Han,[1] Da Mu,[1] Hongfei Song,[1] Ying Meng,[1] Xue Leng,[1] Jinhua Yang,[1] Xu Di,[1] and Qing Chang[2]

[1]*School of Photoelectric Engineering, Changchun university of science and technology, Changchun, 130022, China*
[2] *College of Electronic Engineering, Heilongjiang University, Harbin, 150080, China*
[*]*zhoujhwd@yahoo.com.cn*

Abstract: We present an optical structure, which consists of metal nanoparticles embedded in Fabry-Perot (F-P) cavity, to investigate the Fano resonance, which originates from the interaction between F-P mode and the plasmon modes supported by the nanoparticles. The coupling system is modeled theoretically by coupled-mode theory in time domain and the transmission properties are demonstrated numerically by the finite-difference time-domain method. The charge distribution features of the nanoparticle plasmon modes are further characterized by using boundary integral equation technology. Results show that the F-P modes can be used to active the optical inactive surface plasmon modes by breaking the mode symmetry.

©2013 Optical Society of America

OCIS codes: (250.5403) Plasmonics; (260.5740) Resonance; (350.4238) Nanophotonics and photonic crystals.

References and links

1. B. R. Bułka and P. Stefański, "Fano and Kondo resonance in electronic current through nanodevices," Phys. Rev. Lett. **86**(22), 5128–5131 (2001).
2. K. Kobayashi, H. Aikawa, A. S. Sano, S. Katsumoto, and Y. Iye, "Fano resonance in a quantum wire with a side-coupled quantum dot," Phys. Rev. B **70**(3), 035319 (2004).
3. M. L. Ladron de Guevara, F. Claro, and P. A. Orellana, "Ghost Fano resonance in a double quantum dot molecule attached to leads," Phys. Rev. B **67**(19), 195335 (2003).
4. S. Fan, W. Suh, and J. D. Joannopoulos, "Temporal coupled-mode theory for the Fano resonance in optical resonators," J. Opt. Soc. Am. A **20**(3), 569–572 (2003).
5. M. Kanskar, P. Paddon, V. Pacradouni, R. Morin, A. Busch, J. F. Young, S. R. Johnson, J. MacKenzie, and T. Tiedje, "Observation of leaky slab modes in an air-bridged semiconductor waveguide with a two-dimensional photonic lattice," Appl. Phys. Lett. **70**(11), 1438–1440 (1997).
6. V. N. Astratov, J. S. Culshaw, R. M. Stevenson, D. M. Whittaker, M. S. Skolnick, T. F. Krauss, and R. M. de la Rue, "Resonant coupling of near-infrared radiation to photonic band structure waveguides," J. Lightwave Technol. **17**(11), 2050–2057 (1999).
7. J. B. Lassiter, H. Sobhani, J. A. Fan, J. Kundu, F. Capasso, P. Nordlander, and N. J. Halas, "Fano resonances in plasmonic nanoclusters: geometrical and chemical tunability," Nano Lett. **10**(8), 3184–3189 (2010).
8. N. A. Mirin, K. Bao, and P. Nordlander, "Fano resonances in plasmonic nanoparticle aggregates," J. Phys. Chem. A **113**(16), 4028–4034 (2009).
9. B. Gallinet and O. J. F. Martin, "Influence of electromagnetic interactions on the line shape of plasmonic Fano resonances," ACS Nano **5**(11), 8999–9008 (2011).
10. D. Dregely, M. Hentschel, and H. Giessen, "Excitation and tuning of higher-order Fano resonances in plasmonic oligomer clusters," ACS Nano **5**(10), 8202–8211 (2011).
11. C. Radloff and N. J. Halas, "Plasmonic properties of concentric nanoshells," Nano Lett. **4**(7), 1323–1327 (2004).
12. H. Wang, D. W. Brandl, F. Le, P. Nordlander, and N. J. Halas, "Nanorice: a hybrid plasmonic nanostructure," Nano Lett. **6**(4), 827–832 (2006).
13. F. Hao, C. L. Nehl, J. H. Hafner, and P. Nordlander, "Plasmon resonances of a gold nanostar," Nano Lett. **7**(3), 729–732 (2007).
14. L. Chuntonov and G. Haran, "Trimeric plasmonic molecules: the role of symmetry," Nano Lett. **11**(6), 2440–2445 (2011).
15. H. Wang, Y. Wu, B. Lassiter, C. L. Nehl, J. H. Hafner, P. Nordlander, and N. J. Halas, "Symmetry breaking in individual plasmonic nanoparticles," Proc. Natl. Acad. Sci. U.S.A. **103**(29), 10856–10860 (2006).
16. E. Gómez, K. C. Vernon, and T. J. Davis, "Symmetry effects on the optical coupling between plasmonic nanoparticles with applications to hierarchical structures," Phys. Rev. B **81**(7), 075414 (2010).

#185895 - $15.00 USD Received 25 Feb 2013; revised 9 Apr 2013; accepted 15 Apr 2013; published 10 May 2013
(C) 2013 OSA

17. F. Hao, Y. Sonnefraud, P. V. Dorpe, S. A. Maier, N. J. Halas, and P. Nordlander, "Symmetry breaking in plasmonic nanocavities: subradiant LSPR sensing and a tunable Fano resonance," Nano Lett. **8**(11), 3983–3988 (2008).
18. Y. Cui, J. Zhou, V. A. Tamma, and W. Park, "Dynamic tuning and symmetry lowering of Fano resonance in plasmonic nanostructure," ACS Nano **6**(3), 2385–2393 (2012).
19. J. B. Lassiter, J. Aizpurua, L. I. Hernandez, D. W. Brandl, I. Romero, S. Lal, J. H. Hafner, P. Nordlander, and N. J. Halas, "Close encounters between two nanoshells," Nano Lett. **8**(4), 1212–1218 (2008).
20. W. Rechberger, A. Hohenau, A. Leitner, J. R. Krenn, B. Lamprecht, and F. R. Aussenegg, "Optical properties of two interacting gold nanoparticles," Opt. Commun. **220**(1-3), 137–141 (2003).
21. R. C. Shiu and Y. C. Lan, "Plasmonic Zener tunneling in metal-dielectric waveguide arrays," Opt. Lett. **36**(21), 4179–4181 (2011).
22. A. Taflove and S. C. Hagness, *Computational Electrodynamics: The Finite-Difference Time-Domain Method* (Artech House, 2000).
23. S. F. Mingaleev, A. E. Miroshnichenko, and Y. S. Kivshar, "Coupled-resonator-induced reflection in photonic-crystal waveguide structures," Opt. Express **16**(15), 11647–11659 (2008), http://www.opticsinfobase.org/oe/abstract.cfm?uri=oe-16-15-11647.
24. J. Zhou, D. Mu, J. Yang, W. Han, and X. Di, "Coupled-resonator-induced transparency in photonic crystal waveguide resonator systems," Opt. Express **19**(6), 4856–4861 (2011), http://www.opticsinfobase.org/oe/abstract.cfm?uri=oe-19-6-4856.
25. I. D. Mayergoyz, D. R. Fredkin, and Z. Zhang, "Electrostatic (plasmon) resonances in nanoparticles," Phys. Rev. Lett. **72**, 155412 (2005).
26. D. R. Fredkin and I. D. Mayergoyz, "Resonant behavior of dielectric objects (electrostatic resonances)," Phys. Rev. Lett. **91**(25), 253902 (2003).
27. B. E. Little, S. T. Chu, H. A. Haus, J. Foresi, and J. Laine, "Microring resonator channel dropping filters," J. Lightwave Technol. **15**(6), 998–1005 (1997).
28. J. Zhou, D. Mu, H. Song, X. Leng, Y. Meng, W. Han, J. Yang, X. Di, and Q. Chang, "Plasmon resonances in nanoparticle system consisting of different materials," Opt. Commun. **295**, 235–238 (2013).

1. Introduction

Fano effects, which occur from the interference between a direct and resonance-assisted indirect pathway and exhibit a sharp resonance with a broad background, have been observed in many systems, such as quantum systems [1–3], photonic crystal slab structures [4–6] and plasmonic nanostructures [7–12]. Fano resonance in metal aggregates [7,8], for example, in heptamers, has been intensively studied due to its narrow line width and high sensitivity to structural and environmental parameters, which has great potential for photonic applications. For the aggregates, the collective surface plasmons form superradiant (bright) mode and subradiant (dark) mode and the interference between the two modes exhibits Fano resonance. Many factors affect the Fano resonance of the nanoparticle systems, such as size [8], shapes [11–13], symmetry [14–18] as well as the spacing between particles [19,20]. Recently, we have reported dynamic tuning and symmetry lowering of Fano resonances in gold heptamers fabricated on polydimethylsiloxane (PDMS) by an electron-beam lithography and a lift-off process [18], where Fano resonances arise from the interaction between the superradiant modes and the subradiant modes. In this paper, we theoretically modeled an optical system consisting of metal nanoparticles embedded in Fabry-Perot (F-P) cavity by coupled-mode theory in time domain and numerically demonstrated the Fano resonance by the finite-difference time-domain method. We also characterized the surface plasmon modes of the nanoparticles by using boundary integral equation technology. Results show that optical inactive surface plasmon modes can be excited in such system due to the symmetry breaking by the F-P modes.

2. Theoretical analyze and numerical validation

Figure 1 shows the structure of the Fano resonant system, which consists of metal nanoparticles embedded in the center of the F-P cavity. The nanoparticles are arranged in a square lattice with period $a = 200nm$ and the radius of the particles is 25nm. F-P cavity is formed by dielectric slab sandwiched by two metal films. The dielectric constant of the slab is 6 (e.g. ZnS) and the wavelength dependence of the material refractive index is ignored. Dispersion relation of the metal is described by Drude model

#185895 - $15.00 USD Received 25 Feb 2013; revised 9 Apr 2013; accepted 15 Apr 2013; published 10 May 2013
(C) 2013 OSA

$$\varepsilon = 1 - \frac{\omega_p^2}{\omega^2 + j\,\omega\gamma} \tag{1}$$

where ω represents (angular) frequency, ω_p is the bulk plasma frequency, γ is the collision frequency. The dielectric function of the metal in this model just takes into account the contribution of free electrons and displays a plasma-like dispersion. In the visible wavelength range, it is accurate to describe the optical behavior of noble metals (e.g., silver, gold, copper). In this work, we use the model to describe silver with parameter values $\omega_p = 1.32\times10^{16}\,rad/s$ and $\gamma = 6.8\times10^{13}\,rad/s$ [21].

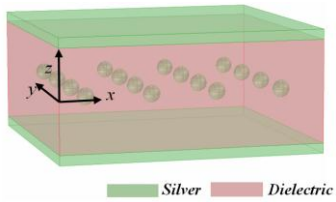

Fig. 1. Structure of Ag nanoparticles embedded in F-P cavity. The F-P cavity is formed by a dielectric slab with two silver films on both sides. The thicknesses of the slab and the silver film are h and $d = 20nm$, respectively. The embedded silver particles, located in the center of the F-P cavity, consist of a square lattice with period $a = 200nm$ and the radii of the particles are 25nm.

To analyze the optical properties of the system, three-dimensional (3D) total-field finite-difference time-domain (FDTD) method is used to calculate the transmission [22]. In the simulation, a single unit cell of the square-lattice array is included with PML absorbing boundary condition on the top and bottom surfaces of the computational domain. For the other four surfaces that are perpendicular to slab, we impose Bloch periodic boundary conditions. A normally incident Gaussian plane-wave pulse (E_x component) is applied to excite the response in the visible wavelength range from a single simulation. The incident plane is placed above the F-P interference. The observation plane is chosen behind the slab. Through direct integration of the Poynting vector over the observation plane, the normalized transmission coefficients are then obtained by Fourier transformation.

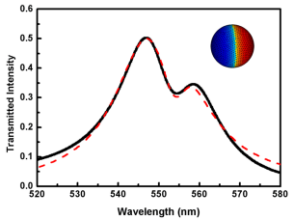

Fig. 2. Transmission of the Fano system with $h = 300nm$. The solid line is obtained by the FDTD method. The dash line is calculated from Eq. (5) with $2/\tau = 5.18\times10^{13}\,rad/s$, $1/\tau_0 = 1.73\times10^{13}\,rad/s$, $1/\tau_1 = 2.16\times10^{13}\,rad/s$, $\omega_0 = 3.43\times10^{15}\,rad/s$, $\mu_1 = 2.10\times10^{13}\,rad/s$, $\omega_1 = 3.40\times10^{15}\,rad/s$. Insertion is the charge distribution of nanosphere dipole mode.

Figure 2 shows the transmission properties of the system, where there is a Fano resonant line shapes superimposed on F-P background. By analyzing the excitation process of the Fano resonance, we know that the incident light excite the F-P mode and then the F-P mode excite plasmon mode of the nanoparticles. So the F-P mode establishes supperradiant state and the plasmon state forms the subradiant state. The interaction between the two types of modes lead the Fano resonance, i.e., in the vicinity of the sub-radiant resonance, a transmittance dip is

#185895 - $15.00 USD Received 25 Feb 2013; revised 9 Apr 2013; accepted 15 Apr 2013; published 10 May 2013
(C) 2013 OSA

introduced on the F-P background line shape by the subradiance. This effect is closely related to the analogue of coupled-resonator-induced reflection [23,24].

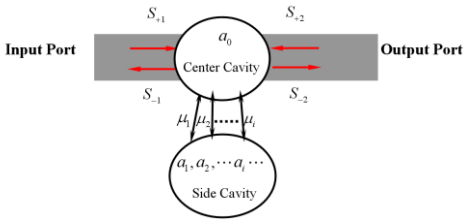

Fig. 3. Illustration of center cavity side-coupled to multi-mode cavity.

In order to obtain a qualitative understanding of Fano resonance in the nanoparticle systems, we provide a theoretical model, as shown in Fig. 3, where the center cavity supports a single supperradiant mode and the side cavity support multi-subradiant modes. The incident optical energy is coupled into the center cavity though the input port, and then the energy in the center cavity couples into the side cavity. Couplings between the modes supported by side cavity are omitted because of orthogonality of the plasmon modes in such a system [25,26]. The amplitude of the center cavity mode and side cavity modes are denoted by a_0 and $a_i\,(i=1,2,\cdots)$ respectively, which are normalized to the energy in the modes. The amplitudes of the incoming and outgoing waves into the center cavity denoted by S_{+j} and S_{-j} ($j=1,2$) (as shown in Fig. 3) and are also normalized to the power carried by the modes. The transmission and reflection properties of such a system can be calculated by the coupled-mode theory in time domain [27]. When the electromagnetic wave at a frequency ω is incident upon the system from the input port, i.e., $S_{+2}=0$, the time evolution of the amplitudes of the cavities in steady state can be described as

$$\frac{da_0}{dt}=j\,\omega_0 a_0-\left(\frac{2}{\tau}+\frac{1}{\tau_0}\right)a_0-\sum_i j\,\mu_i a_i+S_{+1}\sqrt{\frac{2}{\tau}}, \tag{2}$$

$$\frac{da_i}{dt}=j\,\omega_i a_i-\frac{1}{\tau_i}a_i-j\,\mu_i a_0,\ i=1,2,3,\cdots \tag{3}$$

$$S_{-2}=-S_{+2}+j\sqrt{\frac{2}{\tau}}a_0 \tag{4}$$

where ω_0 and ω_i are the center resonant frequencies of the center cavity mode and the i^{th} side cavity mode, respectively. μ_i are the mutual coupling coefficients between the center cavity mode and the i^{th} side cavity mode, $2/\tau$ is the decay rate of the center cavity mode amplitude a_0 into the input and the output ports. $1/\tau_0$ and $1/\tau_i$ are the decay rates of the center cavity mode amplitude and the i^{th} side cavity mode amplitude due to loss, respectively. The transmission of the system can be expressed as

$$T=\left|\frac{S_{-2}}{S_{+1}}\right|^2=\left|\frac{\frac{2}{\tau}}{j\left(\omega-\omega_0\right)+\frac{2}{\tau}+\frac{1}{\tau_0}+\sum_i\frac{\mu_i^2}{j\left(\omega-\omega_i\right)+\frac{1}{\tau_i}}}\right|^2. \tag{5}$$

#185895 - $15.00 USD Received 25 Feb 2013; revised 9 Apr 2013; accepted 15 Apr 2013; published 10 May 2013
(C) 2013 OSA

Examining Eq. (5), if we do not take the loss into account, i.e., $1/\tau_0 = 0$ and $1/\tau_i = 0$, the two-cavity system can be treated as a single composite cavity with the detuning function $\sigma(\omega) = \tau/2[(\omega - \omega_0) - \sum_i \mu_i^2/(\omega - \omega_i)]$ [24], formed by coupling of the center cavity and the side cavity, directly coupled to the input and output ports. Due to the discontinuity of the detuning function at ω_i, the resonant frequency of the composite cavity splits. From Eq. (5), when the detuning function $\sigma(\omega) = 0$, complete transmission can be realized at the frequencies where the center cavity mode splits, i.e. only the F-P mode is excited while the plasmon modes of the nanoparticle are not . It should be emphasized that at resonant frequencies ω_i, where the plasmon modes are excited by the F-P mode, the interaction between the F-P mode and the plamon modes results in the transmission dropping to zero, which is referred as the Fano effect.

For the coupling system with $h = 300nm$, the normal incident light excites an even F-P mode with respect to the center plane of the F-P cavity $z = 0$ around the wavelength 550nm. Then the F-P mode excites the plasmon mode supported by the nanoparticles. It should be note that there is just one plasmon mode (dipole-like mode) around the wavelength. The plamon mode energy coupled back to the F-P mode. The interaction between F-P mode and the plasmon mode splits the F-P mode and leads to Fano resonance. In order to demonstrate the origin of the Fano resonance, simulations of the Fabry-Perot cavity with no silver nanosphere and the silver sphere embedded in a uniform background dielectric of 6 were done at wavelength 544.1nm. Figure 4 shows the slices of the E_x component of the field distribution of the modes at the center plane $y = 0$, where the interaction of the F-P mode and the dipole-like mode results in the Fano resonance. The charge distributions on the nanosphere surface are induced by optical field of the F-P mode, and the field around the nanoparticle is strong and the F-P mode is very weak at the plasmon resonant wavelength 554.1nm. These properties can also be seen from Eq. (2) and (3).

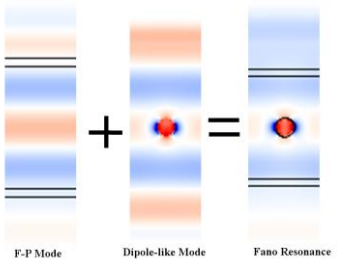

Fig. 4. Steady-state electric field distribution (E_x component at plane $y = 0$) at wavelength $554.1nm$. The red color indicates the field oscillating to right direction and the blue left direction. For F-P mode stimulation, the uniform slab sandwiched between silver films is with same thickness and with an effective dielectric constant. For the dipole-like mode, the silver nanosphere is embedded in a uniform background dielectric of 6.

In order to understand the properties of the plamon modes, which are oscillations of the conduction electrons in metals coupled to the electromagnetic field, boundary integration method [18, 25, 26, 28] was used to determine the charge distribution on the silver nanosphere surface. The insertion in Fig. 2 shows the plasmon mode, which is a dipole-like plasmon mode. The dipole-like plasmon mode emits electromagnetic wave into the F-P cavity. The interaction of the dipole-like plasmon mode with the even F-P mode results in the Fano resonant dip.

In order to further test the validation of the mode analysis provided above, we calculated the transmittance of the system with $h = 360nm$ as shown in Fig. 5(a). Around wavelength 490nm, the nanoparticle supports two plasmon modes. In the vicinity of the wavelength, the

#185895 - $15.00 USD Received 25 Feb 2013; revised 9 Apr 2013; accepted 15 Apr 2013; published 10 May 2013
(C) 2013 OSA

F-P mode is an odd mode, so the plasmon modes are also odd modes. The charge distributions of the two modes are shown in Figs. 5(b) and 5(c). The plasmon mode at wavelength 497.1nm is quadrupole-like mode and octopole-like mode at wavelength 482.8nm. There is no hexapole-like mode excited because of mode symmetry. In general, the whole dipole moments of the quadrupole and the octopole are zero and these plamon modes are optical inactive, but in this system, the F-P mode, which is used to active the plasmon modes, breaks the symmetry and these plasmon modes become optical active and interacted with the F-P mode. Figures 5(d) and 5(e) show the field distributions of the two modes, which are in good agreement with the charge distributions shown in Figs. 5(b) and 5(c), respectively.

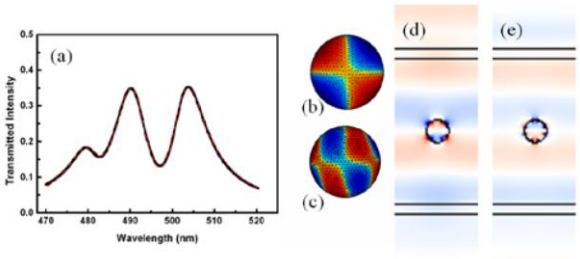

Fig. 5. (a)Transmission of the structure with $h = 360nm$. The solid line is obtained by the FDTD method. The dash curve is calculated from Eq. (5) with $2/\tau = 4.95\times10^{13} rad/s$, $1/\tau_0 = 6.58\times10^{12} rad/s$, $1/\tau_1 = 2.83\times10^{13} rad/s$, $1/\tau_2 = 3.26\times10^{13} rad/s$ $\omega_0 = 3.82\times10^{15} rad/s$, $\mu_1 = 4.70\times10^{13} rad/s$, $\omega_1 = 3.79\times10^{15} rad/s$, $\mu_2 = 3.67\times10^{13} rad/s$, $\omega_2 = 3.90\times10^{15} rad/s$. (b) The charge nanosphere distributions of the quadrupole mode. (c) The charge nanosphere distributions of the octopole mode. (d) and (e) Steady-state electric field distributions (E_x component at plane $y = 0$). (d) Quadrupole-like plasmon mode at wavelength $497.1nm$ (e) Octopole-like plasmon mode at wavelength $482.8nm$.

In the coupling system we proposed, Fano resonance occurs from the interaction between the F-P mode and the plamon modes supported by the metal nanoparticles, where the transmission spectra consist of Fano resonant line shapes superimposed on a smooth F-P background. There are several geometrical parameters that could be directly controllable to improve the tunability of Fano resonance. For example, the change of the F-P cavity length results in the shift of the F-P background line shapes in the spectra, and increase of the metal nanosphere size leads to the Fano resonant dip red-shift due to the retardation effects [18].

3. Conclusion

We investigate the Fano resonance of metal nanoparticles embedded in Fabry-Perot cavity. The optical properties are modeled by coupled-mode theory in time domain and demonstrated by the finite-difference time-domain method. We also analyzed the charge distribution features of the nanoparticle plasmon modes by using boundary integral equation technology. An excellent agreement of plamon mode properties has been found with the present theoretical analysis.

Acknowledgment

This work is supported by National Natural Science Foundation of China (11104020), Sci&Tech Innovation Fund of CUST (XJJLG-2011-07), Heilongjiang province and high-level Team Project of Heilongjiang University(Hdtd2010-15), NSF of Heilongjiang Province (F201032), Heilongjiang Province Postdoctoral Science Foundation (LBH-Q09032).

#185895 - $15.00 USD Received 25 Feb 2013; revised 9 Apr 2013; accepted 15 Apr 2013; published 10 May 2013

(C) 2013 OSA